Peristaltic transport of Johnson–Segalman fluid in a curved channel with compliant walls

Sadia Hina[a], **Tasawar Hayat**[b,c], **Saleem Asghar**[d]

[a]Department of Mathematical Sciences, Fatima Jinnah Women University
Rawalpindi 46000, Pakistan
quaidan85@yahoo.com

[b]Department of Mathematics, Quaid-i-Azam University 45320
Islamabad 44000, Pakistan

[c]Department of Mathematics, Faculty of Science, King Abdulaziz University
Jeddah 21531, Saudi Arabia

[d]Department of Mathematics, COMSATS Institute of Information Technology
Islamabad 44000, Pakistan

Received: 11 Jule 2011 / **Revised:** 24 March 2012 / **Published online:** 5 July 2012

Abstract. The present investigation deals with the peristaltic flow of an incompressible Johnson–Segalman fluid in a curved channel. Effects of the channel wall properties are taken into account. The associated equations for peristaltic flow in a curved channel are modeled. Mathematical analysis is simplified under long wavelength and low Reynolds number assumptions. The solution expressions are established for small Weissenberg number. Effects of several embedded parameters on the flow quantities are discussed.

Keywords: Johnson–Segalman fluid, peristalsis, curved channel.

1 Introduction

The peristaltic flows due to flexible walls of channel/tube are very significant for fluid transport in living organisms and industry. Blood pumps in dialysis and heart lung machine work because of the peristaltic action. In nuclear industry a toxic liquid can be transported by such action in order to avoid contamination of the outside environment. Peristalsis is further responsible for the passage of urine from kidney to bladder, chyme motion in the gastrointestinal tract, blood circulation in small blood vessels, in roller and finger pumps, embryo transport in non-pregnant uterus, etc. Latham [1] and Shapiro et al. [2] presented the seminal works on the peristalsis. Rao and Mishra [3] studied the peristaltic transport of power-law fluid in a porous tube. Peristaltic transport of a Herschel–Bulkley fluid in an inclined tube has been investigated by Vajravelu et al. [4]. Mekheimer and elmaboud [5] studied heat transfer and magnetic field effects on the peristaltic flow

of Newtonian fluid in a vertical annulus. Radhakrishnamacharya and Murty [6] examined the effects of heat transfer on peristaltic transport in a non-uniform channel.

Since most of the fluids in physiology are of non-Newtonian character. Johnson–Segalman fluid is one of the subclass of such viscoelastic fluids. This model has an ability to explain the "spurt" phenomenon. The term "spurt" has been used for the description of large increase in the volume to a small increase in the driving pressure gradient. The peristaltic transport of MHD Johnson–Segalman fluid in a planar channel has been discussed by Hayat et al. [7]. Peristaltic motion of Johnson–Segalman fluid in an asymmetric and planar channel is also studied by Hayat et al. [8]. Nadeem and Akbar [9] studied the peristaltic flow of Johnson–Segalman fluid in a non-uniform tube with heat transfer. In another paper, the same authors examined the heat transfer effects on peristaltic flow of Johnson–Segalman fluid in an inclined asymmetric channel [10]. Induced magnetic field effect is discussed on the peristaltic flow of Johnson Segalman fluid in a vertical symmetric channel by Nadeem and Akbar [11]. Nadeem et al. [12] analyzed the chemical reaction on the peristaltic flow of Johnson Segalman fluid in an endoscope. Akbar et al. [13] studied the slip and heat transfer effects on the peristaltic flow of third order fluid in an inclined asymmetric channel. Peristaltic flow of a Jeffrey-six constant fluid in a diverging tube with heat transfer is studied by Akbar and Nadeem [14]. Tripathi [15] discussed the peristaltic transport of viscoelastic fluid in a channel. Vajravelu et al. [16] studied the influence of heat transfer on peristaltic transport of a Jeffrey fluid in a vertical porous stratum. Hayat et al. [17] analyzed the effects of induced magnetic field on peristaltic flow with heat and mass transfer. Hayat et al. [18] have discussed the MHD peristaltic motion of Johnson–Segalman fluid in a channel with compliant walls. Muthu et al. [19] discussed the peristaltic flow of micropolar fluid in circular cylindrical tubes with wall properties. Elnaby and Haroun [20] reported the effect of wall properties on peristaltic flow in a viscous fluid. Radhakrishnamacharya and Srinivasulu [21] studied the effects of wall properties on peristaltic transport of Newtonian fluid with heat transfer. Hayat et al. [22] looked at the MHD peristaltic flow of Jeffery fluid with compliant walls. Ali et al. [23] have discussed the peristaltic motion of Maxwell fluid with compliant walls. Kothandapani and Srinivas [24] analyzed the influence of wall properties in the MHD peristaltic transport with heat transfer and porous medium. Srinivasacharya et al. [25] discussed the effects of wall Properties on peristaltic transport of a dusty fluid. Srinivas et al. [26] studied the influence of slip conditions, wall properties and heat transfer on MHD peristaltic transport. Sankad and Radharkrishnamacharya [27] discussed the influence of wall properties on the peristaltic motion of a Herschel-Bulkley fluid in a channel. Srinivas and Kothandapani [28] discussed the influence of heat and mass transfer on MHD peristaltic flow of Newtonian fluid in a porous channel with compliant walls. Hayat and Hina [29] examined the heat and mass transfer effects on the MHD peristaltic flow of a Maxwell fluid with wall properties.

Not much has been said about the peristaltic motion in a curved channel. Ali et al. [30] studied the viscous flow analysis in a curved channel. The peristaltic flow in a curved channel with heat transfer is also presented by Ali et al. [31]. Peristaltic flow of third grade fluid in a curved channel is further investigated by Ali et al. [32]. Hayat et al. [33–35] extended the work of Ali et al. [30] for viscous and third grade fluid

in a compliant walls channel respectively. The objective of this investigation is to put forward the analysis of peristaltic flow for a Johnson–Segalman fluid in a curved channel. Hence the Johnson–Segalman fluid in a curved channel with flexible walls is considered. The relevant equations are modeled first time. Series solutions are developed for small Weissenberg number. Graphs for the interesting quantities are plotted and interpreted.

2 Mathematical modelling

Consider a curved channel of uniform thickness $2d_1$ coiled in a circle with centre O and radius R^*. The flow is in the axial direction x and r is the radial direction. The velocity components in the axial and radial directions are respectively denoted by u and v. The shape of walls are

$$r = \pm\eta(x,t) = \pm\left[d_1 + a\sin\frac{2\pi}{\lambda}(x-ct)\right]. \tag{1}$$

In above expression c is the wave speed and a and λ are the wave amplitude and wavelength respectively. The governing equations for the flow analysis can be written as

$$\frac{\partial v}{\partial r} + \frac{R^*}{r+R^*}\frac{\partial u}{\partial x} + \frac{v}{r+R^*} = 0, \tag{2}$$

$$\begin{aligned}\rho\left[\frac{\partial v}{\partial t} + v\frac{\partial v}{\partial r} + \frac{R^*u}{r+R^*}\frac{\partial v}{\partial x} - \frac{u^2}{r+R^*}\right]\\ = -\frac{\partial p}{\partial r} + \frac{1}{r+R^*}\frac{\partial}{\partial r}\big\{(r+R^*)\tau_{rr}\big\} + \frac{R^*}{r+R^*}\frac{\partial \tau_{xr}}{\partial x} - \frac{\tau_{xx}}{r+R^*},\end{aligned} \tag{3}$$

$$\begin{aligned}\rho\left[\frac{\partial u}{\partial t} + v\frac{\partial u}{\partial r} + \frac{R^*u}{r+R^*}\frac{\partial u}{\partial x} + \frac{uv}{r+R^*}\right]\\ = \frac{1}{(r+R^*)^2}\frac{\partial}{\partial r}\big\{(r+R^*)^2\tau_{rx}\big\} + \frac{R^*}{r+R^*}\frac{\partial \tau_{xx}}{\partial x} - \frac{R^*}{r+R^*}\frac{\partial p}{\partial x},\end{aligned} \tag{4}$$

where the constitutive relation for Cauchy stress tensor τ in a Johnson–Segalman fluid is [7]

$$\tau = 2\mu\mathbf{D} + \mathbf{S},$$

where the extra stress tensor $\mathbf{S}$ satisfies

$$\begin{aligned}&\mathbf{S} + m\left[\frac{\mathrm{d}\mathbf{S}}{\mathrm{d}t} + \mathbf{S}(\mathbf{W}-\xi\mathbf{D}) + (\mathbf{W}-\xi\mathbf{D})^{\mathrm{T}}\mathbf{S}\right] = 2\eta_1\mathbf{D},\\ &\mathbf{D} = \frac{1}{2}\big[\operatorname{grad}\mathbf{V} + (\operatorname{grad}\mathbf{V})^{\mathrm{T}}\big],\\ &\mathbf{W} = \frac{1}{2}\big[\operatorname{grad}\mathbf{V} - (\operatorname{grad}\mathbf{V})^{\mathrm{T}}\big].\end{aligned}$$

The above relations imply the following expressions for the extra stress components:

$$S_{rr}+m\left[\frac{\mathrm{d}S_{rr}}{\mathrm{d}t}-\frac{2uS_{rx}}{r+R^*}+S_{rx}\left\{(1-\xi)\frac{\partial u}{\partial r}-\frac{1+\xi}{r+R^*}\left[R^*\frac{\partial v}{\partial x}-u\right]\right\}-2\xi S_{rr}\frac{\partial v}{\partial r}\right]$$
$$=2\eta_1\frac{\partial v}{\partial r}, \tag{5}$$

$$\eta_1\left(\frac{\partial u}{\partial r}+\frac{R^*}{r+R^*}\frac{\partial v}{\partial x}-\frac{u}{r+R^*}\right)$$
$$=S_{rx}+m\frac{\mathrm{d}S_{rx}}{\mathrm{d}t}+\frac{mu(S_{rr}-S_{xx})}{r+R^*}+\frac{mS_{xx}}{2}\left\{(1-\xi)\frac{\partial u}{\partial r}-\frac{1+\xi}{r+R^*}\left[R^*\frac{\partial v}{\partial x}-u\right]\right\}$$
$$+m\frac{S_{rr}}{2}\left\{\frac{1-\xi}{r+R^*}\left[R^*\frac{\partial v}{\partial x}-u\right]-(1+\xi)\frac{\partial u}{\partial r}\right\}, \tag{6}$$

$$S_{xx}+m\left[\frac{\mathrm{d}S_{xx}}{\mathrm{d}t}+\frac{2uS_{rx}}{r+R^*}-S_{rx}\left\{(1+\xi)\frac{\partial u}{\partial r}-\frac{1-\xi}{r+R^*}\left[R^*\frac{\partial v}{\partial x}-u\right]\right\}+2\xi S_{xx}\frac{\partial v}{\partial r}\right]$$
$$=-2\eta_1\frac{\partial v}{\partial r}, \tag{7}$$

where $\mathrm{d}/\mathrm{d}t=\partial/\partial t+v\partial/\partial r+uR^*/(r+R^*)\partial/\partial x$, p the pressure, μ and η_1 are the viscosities, m the relaxation time, ρ the density, R^* the curvature parameter, τ the elastic tension, m_1 the mass per unit area, d the coefficient of viscous damping, $\mathbf{D}$ and $\mathbf{W}$ are the symmetric and skew symmetric parts of velocity gradient, ξ is the slip parameter and S_{xr}, S_{rr} and S_{xx} are the components of an extra stress tensor $\mathbf{S}$.

The boundary conditions can be written as [18, 21–26]

$$u=0 \quad \text{at } r=\pm\eta, \tag{8}$$

$$R^*\left[-\tau\frac{\partial^3}{\partial x^3}+m_1\frac{\partial^3}{\partial x\partial t^2}+d\frac{\partial^2}{\partial t\partial x}\right]\eta$$
$$=\frac{1}{(r+R^*)}\frac{\partial}{\partial r}\left\{(r+R^*)^2\tau_{rx}\right\}+R^*\frac{\partial\tau_{xx}}{\partial x}$$
$$-\rho\big(r+R^*\big)\left[\frac{\partial u}{\partial t}+v\frac{\partial u}{\partial r}+\frac{R^*u}{r+R^*}\frac{\partial u}{\partial x}+\frac{uv}{r+R^*}\right] \quad \text{at } r=\pm\eta. \tag{9}$$

Introducing

$$\psi^*=\frac{\psi}{cd_1},\quad x^*=\frac{x}{\lambda},\quad r^*=\frac{r}{d_1},$$
$$t^*=\frac{ct}{\lambda},\quad \eta^*=\frac{\eta}{d_1},\quad k=\frac{R^*}{d_1},$$
$$p^*=\frac{d_1^2p}{c\lambda(\mu+\eta_1)},\quad S_{ij}^*=\frac{d_1S_{ij}}{c\eta_1},\quad We=\frac{mc}{d_1},$$

Eqs. (5)–(9) take the forms

$$2\frac{\partial v}{\partial r} = S_{rr} + We\left[\left(\delta\frac{\partial}{\partial t} + v\frac{\partial}{\partial r} + \frac{uk\delta}{r+k}\frac{\partial}{\partial x}\right)S_{rr} - \frac{2uS_{rx}}{r+k} - 2\xi S_{rr}\frac{\partial v}{\partial r}\right] + WeS_{rx}\left\{(1-\xi)\frac{\partial u}{\partial r} - \frac{1+\xi}{r+k}\left(k\delta\frac{\partial v}{\partial x} - u\right)\right\}, \tag{10}$$

$$\begin{aligned}&\frac{\partial u}{\partial r} + \frac{k\delta}{r+k}\frac{\partial v}{\partial x} - \frac{u}{r+k}\\ &\quad= S_{rx} + We\left[\left(\delta\frac{\partial}{\partial t} + v\frac{\partial}{\partial r} + \frac{uk\delta}{r+k}\frac{\partial}{\partial x}\right)S_{rx} + \frac{u(S_{rr}-S_{xx})}{r+k}\right]\\ &\qquad+\frac{WeS_{rr}}{2}\left\{\frac{1-\xi}{r+k}\left[k\delta\frac{\partial v}{\partial x} - u\right] - (1+\xi)\frac{\partial u}{\partial r}\right\}\\ &\qquad+\frac{WeS_{xx}}{2}\left\{(1-\xi)\frac{\partial u}{\partial r} - \frac{1+\xi}{r+k}\left[k\delta\frac{\partial v}{\partial x} - u\right]\right\},\end{aligned} \tag{11}$$

$$-2\frac{\partial v}{\partial r} = S_{xx} + We\left[\left(\delta\frac{\partial}{\partial t} + v\frac{\partial}{\partial r} + \frac{uk\delta}{r+k}\frac{\partial}{\partial x}\right)S_{xx} + \frac{2uS_{rx}}{r+k} + 2\xi S_{xx}\frac{\partial v}{\partial r}\right] + WeS_{rx}\left\{\frac{1-\xi}{r+k}\left(k\delta\frac{\partial v}{\partial x} - u\right) - (1+\xi)\frac{\partial u}{\partial r}\right\}, \tag{12}$$

$$\begin{aligned}&Re\,\delta\left[\delta\frac{\partial v}{\partial t} + v\frac{\partial v}{\partial r} + \frac{k\delta u}{r+k}\frac{\partial v}{\partial x} - \frac{u^2}{r+k}\right]\\ &\quad= -\frac{\eta_1+\mu}{\eta_1}\frac{\partial p}{\partial r} + \frac{4\delta\mu}{\eta_1(r+k)}\frac{\partial v}{\partial r} + \frac{k\delta^3}{r+k}\frac{\partial S_{rx}}{\partial x} + \delta\frac{\partial S_{rr}}{\partial r} + \frac{\delta(S_{rr}-S_{xx})}{r+k}\\ &\qquad+\frac{\delta\mu}{\eta_1}\frac{\partial^2 v}{\partial r^2} + \frac{\delta^2 k\mu}{\eta_1(k+r)}\frac{\partial}{\partial x}\left(\frac{\partial u}{\partial r} + \frac{k\delta}{r+k}\frac{\partial v}{\partial x} - \frac{u}{r+k}\right),\end{aligned} \tag{13}$$

$$\begin{aligned}&Re\left[\delta\frac{\partial u}{\partial t} + v\frac{\partial u}{\partial r} + \frac{k\delta u}{r+k}\frac{\partial u}{\partial x} + \frac{uv}{r+k}\right]\\ &\quad= -\frac{(\eta_1+\mu)k}{\eta_1(r+k)}\frac{\partial p}{\partial x} + \frac{\partial S_{rx}}{\partial r} + \frac{2S_{rx}}{r+k} + \frac{k\delta}{r+k}\frac{\partial S_{xx}}{\partial x}\\ &\qquad-\frac{2k\delta\mu}{(r+k)\eta_1}\frac{\partial^2 v}{\partial r\partial x} + \frac{\mu}{\eta_1}\frac{\partial}{\partial r}\left(\frac{\partial u}{\partial r} + \frac{k\delta}{r+k}\frac{\partial v}{\partial x} - \frac{u}{r+k}\right)\\ &\qquad+\frac{2\mu}{\eta_1(r+k)}\left(\frac{\partial u}{\partial r} + \frac{k\delta}{r+k}\frac{\partial v}{\partial x} - \frac{u}{r+k}\right).\end{aligned} \tag{14}$$

The boundary conditions now reduce to the following expressions:

$$u = 0 \quad \text{at } r = \pm\eta = \pm\big(1 + \epsilon\sin 2\pi(x-t)\big), \tag{15}$$

$$k\left[E_1\frac{\partial^3}{\partial x^3}+E_2\frac{\partial^3}{\partial x\partial t^2}+E_3\frac{\partial^2}{\partial t\partial x}\right]\eta$$
$$=\frac{\eta_1(r+k)}{(\eta_1+\mu)}\left[\frac{\partial}{\partial r}\left(\frac{\partial u}{\partial r}+\frac{k\delta}{r+k}\frac{\partial v}{\partial x}-\frac{u}{r+k}\right)-\frac{2k\delta}{r+k}\frac{\partial^2 v}{\partial r\partial x}\right]$$
$$-\frac{Re\mu(r+k)}{(\eta_1+\mu)}\left[\delta\frac{\partial u}{\partial t}+v\frac{\partial u}{\partial r}+\frac{k\delta u}{r+k}\frac{\partial u}{\partial x}+\frac{uv}{r+k}\right]$$
$$+\frac{\eta_1(r+k)}{(\eta_1+\mu)}\left[\frac{\partial S_{rx}}{\partial r}+\frac{2S_{rx}}{r+k}+\frac{k\delta}{r+k}\frac{\partial S_{xx}}{\partial x}\right]$$
$$+\frac{2\mu}{(\eta_1+\mu)}\left(\frac{\partial u}{\partial r}+\frac{k\delta}{r+k}\frac{\partial v}{\partial x}-\frac{u}{r+k}\right)\quad\text{at } r=\pm\eta. \tag{16}$$

Obviously the continuity equation (2) is satisfied identically, ϵ $(=a/d_1)$, δ $(=d_1/\lambda)$ the geometric parameters, k the dimensionless curvature parameter, Re $(=c\rho d_1/\eta_1)$ the Reynolds number and E_1 $(=-\tau d_1^3/\lambda^3\eta_1 c)$, E_2 $(=m_1 c d_1^3/\lambda^3\eta_1)$, E_3 $(=d d_1^3/\lambda^2\eta_1)$ the non-dimensional elasticity parameters [16,18,21-26].

If $\psi(x,y,t)$ is the stream function then writing

$$u=-\frac{\partial\psi}{\partial r},\quad v=\delta\frac{k}{k+r}\frac{\partial\psi}{\partial x},$$

expressions (10)–(16) after using long wavelength and low Reynolds number assumptions give

$$\frac{\partial p}{\partial r}=0, \tag{17}$$

$$-\frac{k(\eta_1+\mu)}{\eta_1(r+k)}\frac{\partial p}{\partial x}+\frac{\partial S_{rx}}{\partial r}+\frac{2S_{rx}}{r+k}+\frac{\mu}{\eta_1}\frac{\partial}{\partial r}\left(-\psi_{rr}+\frac{\psi_r}{r+k}\right)$$
$$+\frac{2\mu}{(r+k)\eta_1}\left(-\psi_{rr}+\frac{\psi_r}{r+k}\right)=0, \tag{18}$$

$$\psi_r=0\quad\text{at } r=\pm\eta=\pm\big(1+\epsilon\sin 2\pi(x-t)\big), \tag{19}$$

$$k\left[E_1\frac{\partial^3}{\partial x^3}+E_2\frac{\partial^3}{\partial x\partial t^2}+E_3\frac{\partial^2}{\partial t\partial x}\right]\eta$$
$$=\frac{\eta_1(r+k)}{(\eta_1+\mu)}\left[\frac{\mu}{\eta_1}\frac{\partial}{\partial r}\left(-\psi_{rr}+\frac{\psi_r}{r+k}\right)+\frac{\partial S_{rx}}{\partial r}+\frac{2S_{rx}}{r+k}\right]$$
$$+\frac{2\mu}{(\eta_1+\mu)}\left(-\psi_{rr}+\frac{\psi_r}{r+k}\right)\quad\text{at } r=\pm\eta \tag{20}$$

with

$$0=S_{rr}+WeS_{rx}\left[-(1-\xi)\psi_{rr}-\frac{1+\xi}{r+k}\psi_r+\frac{2\psi_r}{r+k}\right], \tag{21}$$

$$-\psi_{rr}+\frac{\psi_r}{r+k}=-We\frac{\psi_r(S_{rr}-S_{xx})}{r+k}+\frac{WeS_{rr}}{2}\left\{\frac{1-\xi}{r+k}\psi_r+(1+\xi)\psi_{rr}\right\}$$
$$+S_{rx}-\frac{WeS_{xx}}{2}\left\{(1-\xi)\psi_{rr}+\frac{1+\xi}{r+k}\psi_r\right\}, \tag{22}$$

$$0=S_{xx}+WeS_{rx}\left[-\frac{2\psi_r}{r+k}+\left\{\frac{1-\xi}{r+k}\psi_r+(1+\xi)\psi_{rr}\right\}\right]. \tag{23}$$

From Eqs. (21)–(23) we can write

$$S_{rx}=\left(-\psi_{rr}+\frac{\psi_r}{r+k}\right)\left[1+We^2\big(1-\xi^2\big)\left(-\psi_{rr}+\frac{\psi_r}{r+k}\right)^2\right]^{-1}. \tag{24}$$

With the help of Eqs. (17)–(18) one obtains

$$(k+r)\frac{\partial^2 S_{rx}}{\partial r^2}+3\frac{\partial S_{rx}}{\partial r}+\frac{(k+r)\mu}{\eta_1}\frac{\partial^2}{\partial r^2}\left(-\psi_{rr}+\frac{\psi_r}{r+k}\right)$$
$$+\frac{3\mu}{\eta_1}\frac{\partial}{\partial r}\left(-\psi_{rr}+\frac{\psi_r}{r+k}\right)=0. \tag{25}$$

3 Solution methodology

In order to proceed for the series solution we write

$$\psi=\psi_0+We^2\psi_1+We^4\psi_2+\ldots, \tag{26}$$
$$S_{rx}=S_{0rx}+We^2S_{1rx}+We^4S_{2rx}+\ldots. \tag{27}$$

3.1 Zeroth order system

Substituting Eqs. (26) and (27) into Eqs. (19)–(20) and (24)–(25) and then equating the coefficients of We^0 we have

$$(k+r)\frac{\partial^2}{\partial r^2}\left(-\psi_{0rr}+\frac{\psi_{0r}}{r+k}\right)+3\frac{\partial}{\partial r}\left(-\psi_{0rr}+\frac{\psi_{0r}}{r+k}\right)=0, \tag{28}$$

$$\psi_{0r}=0 \quad \text{at } r=\pm\eta, \tag{29}$$

$$k\left[E_1\frac{\partial^3}{\partial x^3}+E_2\frac{\partial^3}{\partial x\partial t^2}+E_3\frac{\partial^2}{\partial t\partial x}\right]\eta$$
$$=(k+r)\frac{\partial}{\partial r}\left(-\psi_{0rr}+\frac{\psi_{0r}}{r+k}\right)+2\left(-\psi_{0rr}+\frac{\psi_{0r}}{r+k}\right) \quad \text{at } r=\pm\eta. \tag{30}$$

The solution of above equations can be written as

$$\psi_0=C_1+C_2\ln(r+k)+C_3(r+k)^2+C_4(r+k)^2\ln(r+k), \tag{31}$$

while the velocity expression at this order is

$$u_0 = -\psi_{0r} = -\frac{C_2}{r+k} - 2C_3(r+k) - C_4(r+k)\big\{1+2\ln(r+k)\big\}, \tag{32}$$

$$C_1 = -C_2\ln k - C_3k^2 - C_4k^2\ln k,$$
$$C_2 = \frac{C_4}{2k\eta}\big(k^2-\eta^2\big)^2\ln\bigg(\frac{k+\eta}{k-\eta}\bigg),$$
$$C_3 = -\frac{C_4}{4k\eta}\big\{2k\eta + (k+\eta)^2\ln(k+\eta) - (k-\eta)^2\ln(k-\eta)\big\},$$
$$C_4 = -2\epsilon\pi^3k\bigg\{\frac{E_3}{2\pi}\sin 2\pi(x-t) - (E_1+E_2)\cos 2\pi(x-t)\bigg\}.$$

3.2 First order system

The coefficients of $O(We^2)$ leads to the following expressions:

$$0 = (k+r)\frac{\partial^2}{\partial r^2}\bigg[\bigg(-\psi_{1rr}+\frac{\psi_{1r}}{r+k}\bigg) - \frac{(1-\xi^2)\eta_1}{(\eta_1+\mu)}\bigg(-\psi_{0rr}+\frac{\psi_{0r}}{r+k}\bigg)^3\bigg]$$
$$+3\frac{\partial}{\partial r}\bigg[\bigg(-\psi_{1rr}+\frac{\psi_{1r}}{r+k}\bigg) - \frac{(1-\xi^2)\eta_1}{(\eta_1+\mu)}\bigg(-\psi_{0rr}+\frac{\psi_{0r}}{r+k}\bigg)^3\bigg], \tag{33}$$

$$\psi_{1r} = 0 \quad \text{at } r = \pm\eta, \tag{34}$$

$$0 = (k+r)\frac{\partial}{\partial r}\bigg[\bigg(-\psi_{1rr}+\frac{\psi_{1r}}{r+k}\bigg) - \frac{(1-\xi^2)\eta_1}{(\eta_1+\mu)}\bigg(-\psi_{0rr}+\frac{\psi_{0r}}{r+k}\bigg)^3\bigg]$$
$$+2\frac{\partial}{\partial r}\bigg[\bigg(-\psi_{1rr}+\frac{\psi_{1r}}{r+k}\bigg) - \frac{(1-\xi^2)\eta_1}{(\eta_1+\mu)}\bigg(-\psi_{0rr}+\frac{\psi_{0r}}{r+k}\bigg)^3\bigg] \quad \text{at } r = \pm\eta. \tag{35}$$

Inserting the solution expressions at the zeroth order into first order system and then solving the resulting problems we have

$$\psi_1 = C_{11} + C_{12}\ln(r+k) + C_{13}(r+k)^2 + C_{14}(r+k)^2\ln(r+k)$$
$$+\frac{(1-\xi^2)\eta_1C_2^2}{(\eta_1+\mu)}\bigg\{\frac{3C_4}{(r+k)^2} - \frac{C_2}{3(r+k)^4}\bigg\}, \tag{36}$$

$$u_1 = -\psi_{1r} = -\frac{C_{12}}{r+k} - 2C_{13}(r+k) - C_{14}(r+k)\big\{1+2\ln(r+k)\big\}$$
$$-\frac{(1-\xi^2)\eta_1C_2^2}{(\eta_1+\mu)}\bigg\{\frac{6C_4}{(r+k)^3} - \frac{4C_2}{3(r+k)^5}\bigg\}, \tag{37}$$

$$C_{11} = -C_{12}\ln k - C_{13}k^2 - C_{14}k^2\ln k + \frac{6C_2^2C_4}{k^2} - \frac{2C_2^3}{3k^4},$$

$$C_{12} = \left[3C_4\left\{\frac{k-\eta}{(k+\eta)^3} - \frac{k+\eta}{(k-\eta)^3}\right\} - \frac{2C_2}{3}\left\{\frac{k-\eta}{(k+\eta)^5} - \frac{k+\eta}{(k-\eta)^5}\right\}\right]$$
$$\times\frac{\eta_1(1-\xi^2)(k^2-\eta^2)C_2^2}{2k\eta(\eta_1+\mu)} + \frac{C_{14}}{2k\eta}\left(k^2-\eta^2\right)^2\ln\left(\frac{k+\eta}{k-\eta}\right),$$
$$C_{13} = \frac{\eta_1(1-\xi^2)C_2^2}{4k\eta(\eta_1+\mu)}\left[\frac{2C_2}{3}\left\{\frac{1}{(k+\eta)^4} - \frac{1}{(k-\eta)^4}\right\} - 3C_4\left\{\frac{1}{(k+\eta)^2} - \frac{1}{(k-\eta)^2}\right\}\right]$$
$$-\frac{C_{14}}{4k\eta}\left[(k+\eta)^2\ln(k+\eta) - (k-\eta)^2\ln(k-\eta) + 2k\eta\right],$$
$$C_{14} = \frac{4\eta_1(1-\xi^2)C_4^3}{(\eta_1+\mu)},$$

where C_1 and C_{11} are obtained by the condition $\psi(0) = 0$.

4 Results and discussion

This section provides the variation of the various parameters on the axial velocity $u = u_0 + We^2u_1 = -\psi_{0y} - We^2\psi_{1y}$ and stream function ψ. In particular, the role of compliant wall parameters, i.e. E_1 the elastic tension in the membrane, E_2 the mass per unit area, E_3 the coefficient of viscous damping, amplitude ratio ϵ, curvature parameter k, Weissenberg number We and slip parameter ξ have been explained.

Fig. 1 shows the behavior of parameters involved in the axial velocity u. Figs. 1(a) and 1(b) indicate that the axial velocity increases by increasing We. Physically, the increase of Weissenberg number corresponds to growth of relaxation time and decay of viscosity that's why the velocity increases with We. These figures also show that velocity in Johnson–Segalman fluid is larger when compared with the Newtonian fluid. Fig. 1(a) is for small curvature and the axial velocity is not symmetric about the centre line of the channel. Fig. 1(b) is for We with large value of curvature parameter (straight channel). It can be seen that the axial velocity is symmetric about the centre line of the channel (Fig. 1(b)). Figs. 1(c) and 1(d) describe the behavior of slip parameter ξ on the axial velocity. These figures indicate that velocity decreases by increasing ξ. It is noticed that the large curvature shifts the curved channel into straight channel that's why Fig. 1(d) is symmetric about centre line which is for straight channel whereas Fig. 1(c) is tilted towards left i.e. the lower part of the channel. The compliant wall effects (E_1, E_2 and E_3) on the velocity are sketched in the Figs. 1(e) and 1(f). It is found that velocity decreases with an increase in E_3. From physical point of view E_3 represents the oscillatory resistance due to which the velocity decreases. The axial velocity is increasing function of E_1 and E_2. Fig. 1(e) is for curved channel. The velocity profile is not symmetric about the centre line whereas for straight channel, i.e. for large curvature parameter, the velocity profile is symmetric about the centre line of the channel. Fig. 1(g) shows that the axial velocity decreases near the lower wall of the channel and increases in the rest part of the channel when there is an increase in the curvature parameter k. The point of maxima where the velocity is maximum decreases in magnitude in the curved channel.

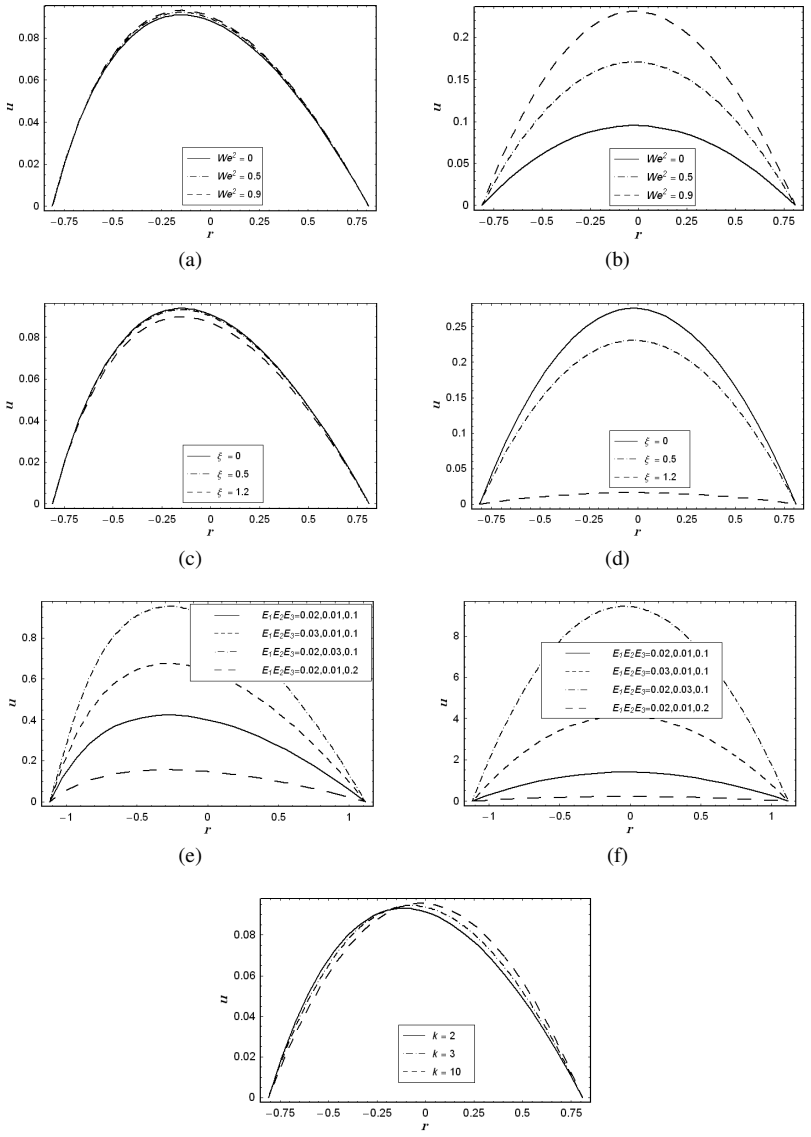

Fig. 1. Variation of We^2 on u when $E_1 = 0.02$, $E_2 = 0.01$, $E_3 = 0.1$, $\epsilon = 0.2$, $\eta_1 = 0.1$, $\mu = 0.1$, $\xi = 0.5$, $x = -0.2$, $t = 0.1$: (a) $k = 1.5$, (b) $k = 10$. Variation of ξ on u when $E_1 = 0.02$, $E_2 = 0.01$, $E_3 = 0.1$, $\epsilon = 0.2$, $We^2 = 0.9$, $\mu = 0.2$, $\eta_1 = 0.2$, $x = -0.2$, $t = 0.1$: (c) $k = 1.5$, (d) $k = 10$. Variation of compliant wall parameters on u when $\eta_1 = 0.1$, $\epsilon = 0.2$, $We^2 = 0.2$, $\mu = 0.1$, $\xi = 0.5$, $x = 0.2$, $t = 0.1$: (e) $k = 1.5$, (f) $k = 10$. Variation of k on u when $E_1 = 0.02$, $E_2 = 0.01$, $E_3 = 0.1$, $\epsilon = 0.2$, $We^2 = 0.01$, $\xi = 0.5$, $\mu = 0.1$, $\eta_1 = 0.1$, $x = -0.2$, $t = 0.1$ (g).

Figs. 2–5 indicate the behavior of parameters in the stream function. Fig. 2 shows that the bolus increases with an increase in We. Physically, Weissenberg number is the ratio of the fluid's relaxation time to the flow's characteristic time so by increasing We the viscosity decreases and the size of trapped bolus increases. From this figure we can conclude that the bolus size increases for Johnson–Segalman fluid in comparison to Newtonian fluid. Fig. 3 shows that the size of bolus decreases with the slip parameter. Fig. 4 is plotted to study the behavior of curvature parameter. This figure shows that the size of bolus increases when k increase. The size of trapped bolus is not similar in the upper and lower parts of the channel which is due to the curvature effects whereas the size of trapped bolus become symmetric about the central line in the planar channel. Figs. 5(a)–5(c) show that the size of trapped bolus increases when E_1 and E_2 increase because these are the elastance parameters that increases the velocity as well as the size of trapped bolus. Figs. 5(a) and 5(d) depict that bolus size decreases when there is an increase in E_3 i.e. the increase in oscillatory resistance decreases the size of bolus.

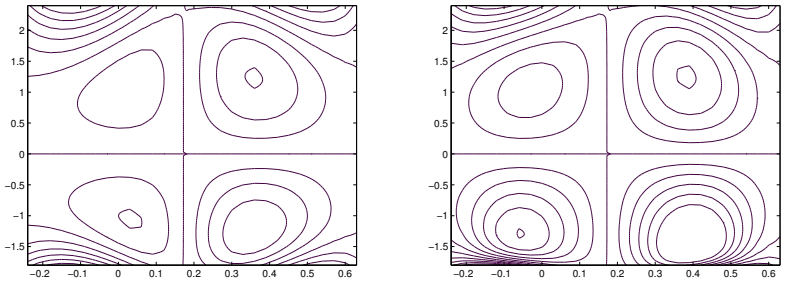

(a) (b)

Fig. 2. Variation of We^2 on ψ when $E_1 = 0.02$, $E_2 = 0.01$, $E_3 = 0.1$, $\epsilon = 0.3$, $t = 0$, $\xi = 0.1$, $k = 2.5$, $\eta_1 = 0.1$, $\mu = 0.1$: (a) $We^2 = 0$, (b) $We^2 = 0.02$.

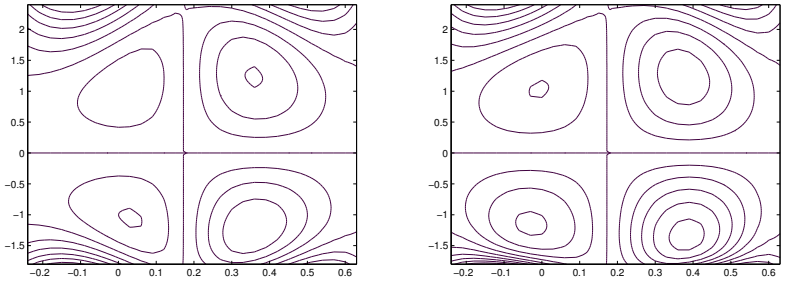

(a) (b)

Fig. 3. Variation of ξ on ψ when $E_1 = 0.02$, $E_2 = 0.01$, $E_3 = 0.1$, $\epsilon = 0.3$, $t = 0$, $We^2 = 0.1$, $k = 2.5$, $\eta_1 = 0.1$, $\mu = 0.1$: (a) $\xi = 0.1$, (b) $\xi = 0.6$.

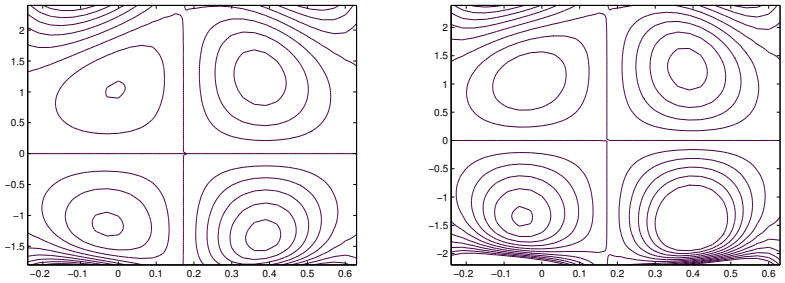

(a) (b)

Fig. 4. Variation of k on ψ when $E_1 = 0.02$, $E_2 = 0.01$, $E_3 = 0.1$, $\epsilon = 0.3$, $t = 0$, $We^2 = 0.1$, $\xi = 0.1$, $\eta_1 = 0.1$, $\mu = 0.1$: (a) $k = 2.5$, (b) $k = 3$.

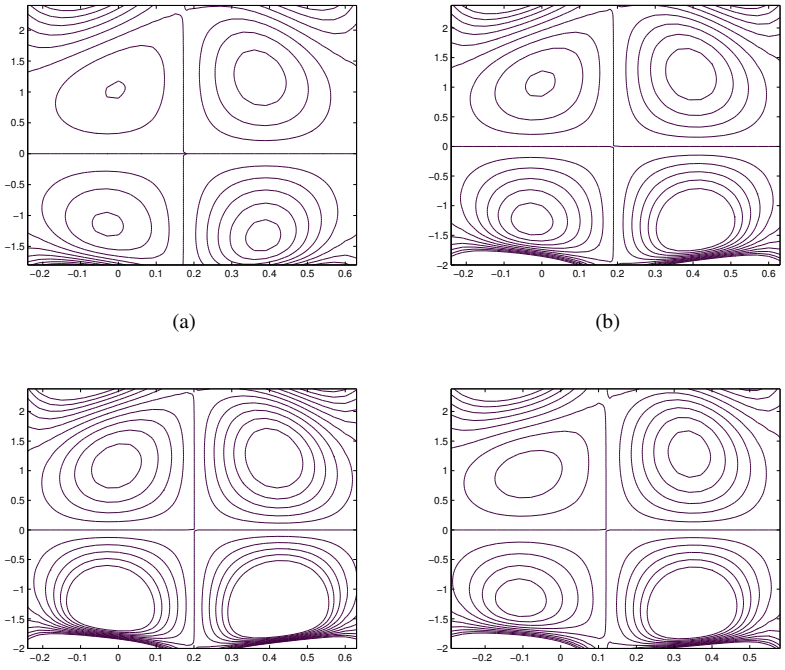

(a) (b)

(c) (d)

Fig. 5. Variation of compliant wall parameters on ψ when $\eta_1 = 0.1$, $\xi = 0.1$, $\epsilon = 0.3$, $t = 0$, $We^2 = 0.1$, $k = 2.5$, $\mu = 0.1$: (a) $E_1 = 0.02$, $E_2 = 0.01$, $E_3 = 0.1$; (b) $E_1 = 0.03$, $E_2 = 0.01$, $E_3 = 0.1$; (c) $E_1 = 0.02$, $E_2 = 0.03$, $E_3 = 0.1$; (d) $E_1 = 0.02$, $E_2 = 0.01$, $E_3 = 0.2$, $k = 2.5$.

5 Concluding remarks

The peristaltic flow of Johnson–Segalman fluid in a curved channel is discussed. Present analysis has been performed under the long wavelength and low Reynolds number approximations. It is observed that the axial velocity in Johnson–Segalman fluid is larger than the Newtonian fluid. Due to curved channel the velocity profile is tilted towards left. The curved channel for large curvature parameter is reduced into the straight channel. This fact is also obvious from the modeled equations. The slip parameter decrease the velocity profile. The bolus size in Johnson–Segalman fluid is greater than the viscous fluid. In curved channel, there is no symmetry in the bolus in the upper and lower halves of the channel. We can reduce this problem for upper convected Maxwell fluid model by taking $\xi = 1$ and $\mu = 0$ and in Newtonian fluid model by considering $m = \mu = 0$.

References

1. T.W. Latham, *Fluid Motion in a Peristaltic Pump*, MS Thesis, MIT Cambridge MA, 1966.
2. M.Y. Jaffrin, A.H. Shapiro, Peristaltic pumping, *Annu. Rev. Fluid Mech.*, **3**, pp. 13–16, 1971.
3. A.R. Rao, M. Mishra, Peristaltic transport of a power-law fluid in a porous tube, *J. Non-Newton. Fluid Mech.*, **121**, pp. 163–174, 2004.
4. K. Vajravelu, G. Radhakrishnamacharya, V.R. Murty, Peristaltic transport of a Herschel–Bulkley fluid in an inclined tube, *Int. J. Non-Linear Mech.*, **40**, pp. 83–90, 2005.
5. Kh.S. Mekheimer, Y. Abd elmaboud, The influence of heat transfer and magnetic field on peristaltic transport of a Newtonian fluid in a vertical annulus: Application of an endoscope, *Phys. Lett., A*, **372**, pp. 1657–1665, 2008.
6. G. Radhakrishnamacharya, V.R. Murty, Heat transfer to peristaltic transport in a non-uniform channel, *Def. Sci. J.*, **43**, pp. 275–280, 1993.
7. T. Hayat, F.M. Mahomed, S. Ashgar, Peristaltic flow of a magnetohydrodynamic Johnson–Segalman fluid, *Nonlinear Dyn.*, **40**, pp. 375–385, 2005.
8. T. Hayat, A. Afsar, N. Ali, Peristaltic transport of a Johnson–Segalman fluid in an asymmetric channel, *Math. Comput. Modelling*, **47**, pp. 380–400, 2008.
9. S. Nadeem, N.S. Akbar, Influence of heat transfer on a peristaltic flow of Johnson–Segalman fluid in a non uniform tube, *Int. Commun. Heat Mass Transfer*, **36**, pp. 1050–1059, 2009.
10. S. Nadeem, N.S. Akbar, Influence of heat transfer on peristaltic transport of a Johnson–Segalman fluid in an inclined asymmetric channel, *Commun. Nonlinear Sci. Numer. Simul.*, **15**, pp. 2860–2877, 2010.
11. S. Nadeem, N.S. Akbar, Effects of induced magnetic field on the peristaltic flow of Johnson Segalman fluid in a vertical symmetric channel, *Appl. Math. Mech.*, **31**, pp. 1–10, 2010.
12. S. Ndeem, N.S. Akbar, S. Ashiq, Simulation of heat and chemical reactions on the peristaltic flow of a Johnson Segalman fluid in an endoscope, *Int. J. Nonlinear Sci. Numer. Simul.*, **11**, pp. 871–883, 2010.

13. N.S. Akbar, T. Hayat, S. Nadeem, A.A. Hendi, Effects of slip and heat transfer on the peristaltic flow of a third order fluid in an inclined asymmetric channel, *Int. J. Heat Mass Transfer*, **54**, pp. 1654–1664, 2011.

14. N.S. Akbar, S. Nadeem, Simulation of heat transfer on the peristaltic flow of a Jeffrey-six constant fluid in a diverging tube, *Int. Commun. Heat Mass Transfer*, **38**, pp. 154–159, 2011.

15. D. Tripathi, Peristaltic transport of a viscoelastic fluid in a channel, *Acta Astron.*, **68**, pp. 1379 – 1385, 2011.

16. K. Vajravelu, S. Sreenadh, P. Lakshminarayana, The influence of heat transfer on peristaltic transport of a Jeffrey fluid in a vertical porous stratum, *Commun. Nonlinear Sci. Numer. Simul.*, **16**, pp. 3107–3125, 2011.

17. T. Hayat, S. Noreen, M.S. Alhothualib, S. Asghar, A. Alhomaidan, Peristaltic flow under the effects of an induced magnetic field and heat and mass transfer, *Int. J. Heat Mass Tranfer*, **55**, pp. 443–452, 2012.

18. T. Hayat, M. Javed, S. Asghar, MHD peristaltic motion of Johnson–Segalman fluid in a channel with compliant walls, *Phys. Lett., A*, **372**, pp. 5026–5036, 2008.

19. P. Muthu, B.V.R. Kumar, P. Chandra, Peristaltic motion of micropolar fluid in circular cylindrical tubes: Effect of wall properties, *Appl. Math. Modelling*, **32**, pp. 2019–2033, 2008.

20. M.A. Abd Elnaby, M.H. Haroun, A new model for study the effect of wall properties on peristaltic transport of a viscous fluid, *Commun. Nonlinear Sci. Numer. Simul.*, **13**, pp. 752–762, 2007.

21. G. Radhakrishnamacharya, C. Srinivasulu, Influence of wall properties on peristaltic transport with heat transfer, *C. R., Méc., Acad. Sci. Paris*, **335**, pp. 369–373, 2007.

22. T. Hayat, M. Javed, N. Ali, MHD peristaltic transport of Jeffery fluid in a channel with compliant walls and porous space, *Transp. Porous Media*, **74**, pp. 259–274, 2008.

23. N. Ali, T. Hayat, S. Asghar, Peristaltic flow of a Maxwell fluid in a channel with compliant walls, *Chaos Solitons Fractals*, **39**, pp. 407–416, 2009.

24. M. Kothandapani, S. Srinivas, On the influence of wall properties in the MHD peristaltic transport with heat transfer and porous medium, *Phys. Lett., A*, **372**, pp. 4586–4591, 2008.

25. D. Srinivasacharya, G. Radhakrishnamacharya, Ch. Srinivasulu, The effects of wall Properties on peristaltic transport of a dusty fluid, *Turk. J. Eng. Environ. Sci.*, **32**, pp. 357–365, 2008.

26. S. Srinivas, R. Gayathri, M. Kothandapani, The influence of slip conditions, wall properties and heat transfer on MHD peristaltic transport, *Comput. Phys. Commun.*, **180**, pp. 2115–2122, 2009.

27. G.C. Sankad, G. Radharkrishnamacharya, Influence of wall properties on the peristaltic motion of a Herschel–Bulkley fluid in a channel, *ARPN J. Eng. Appl. Sci.*, **10**, pp. 27–35, 2009.

28. S. Srinivas, M. Kothandapani, The influence of heat and mass transfer on MHD peristaltic flow through a porous space with compliant walls, *Appl. Math. Comput.*, **213**, pp. 197–208, 2009.

29. T. Hayat, S. Hina, The influence of wall properties on the MHD peristaltic flow of a Maxwell fluid with heat and mass transfer, *Nonlinear Anal., Real World Appl.*, **11**, pp. 3155–3169, 2010.

30. N. Ali, M. Sajid, T. Hayat, Long wavelength flow analysis in a curved channel, *Z. Naturforsch., A*, **65**, pp. 191–196, 2010.

31. N. Ali, M. Sajid, T. Javed, Z. Abbas, Heat transfer analysis of peristaltic flow in a curved channel, *Int. J. Heat Mass Transfer*, **53**, pp. 3319–3325, 2010.

32. N. Ali, M. Sajid, Z. Abbas, T. Javed, Non-Newtonian fluid flow induced by peristaltic waves in a curved channel, *Eur. J. Mech., B, Fluids*, **29**, pp. 387–394, 2010.

33. T. Hayat, M. Javed, A.A. Hendi, Peristaltic transport of viscous fluid in a curved channel with compliant walls, *Int. J. Heat Mass Transfer*, **54**, pp. 1615–1621, 2011.

34. T. Hayat, S. Hina, M. Mustafa, A.A. Hendi, S. Asghar, Effect of wall properties on the peristaltic flow of a third grade fluid in a curved channel, *J. Mech. Med. Biol.*, 2012, doi: 10.1142/S0219519412500674.

35. T. Hayat, S. Hina, A.A. Hendi, S. Asghar, Effect of wall properties on the peristaltic flow of a third grade fluid in a curved channel with heat and mass transfer, *Int. J. Heat Mass Transfer*, **54**, pp. 5126–5136, 2011.